Halo Growth of Proton Beams in Nonlinear Lattices

IOTA/FAST Collaboration Meeting

Oct. 27-29, 2021

Chad Mitchell*
Lawrence Berkeley National Laboratory

*work done with K. Hwang (MSU) and R. Ryne (LBNL)
Thanks to collaborators at FNAL and RadiaSoft

BERKELEY LAB

U.S. DEPARTMENT OF ENERGY | Office of Science

ACCELERATOR TECHNOLOGY & APPLIED PHYSICS DIVISION ATAP

Outline

- *Space charge in the IOTA nonlinear integrable lattice*
- *Structure of the high-intensity proton beam*
  - *adiabatic matching procedure*
  - *constant focusing equilibria*
- *Halo formation and diffusion at high intensity*
  - *simulation results for 5 mA and 8 mA*
  - *possible diffusion mechanisms*
- *Mitigation through nonlinear magnet design*
- *Conclusions*

- Space charge in the IOTA nonlinear integrable lattice

Nonlinear Integrable Optics Lattice Configuration

- **Dynamics inside the nonlinear magnetic insert:**

$$H_\perp = \frac{1}{2}(P_x^2 + P_y^2) - \frac{\tau c^2}{\beta(s)} U\left(\frac{X}{c\sqrt{\beta(s)}}, \frac{Y}{c\sqrt{\beta(s)}}\right) \Rightarrow H_N = \frac{1}{2}(P_{xN}^2 + P_{yN}^2 + X_N^2 + Y_N^2) - \tau U(X_N, Y_N)$$

first invariant

Courant-Snyder transformation, scaling

D&N give in [1] a realizable potential U such that H_N admits a second invariant I_N :

$$\{H_N, I_N\} = 0 \cdot$$

- **Dynamics in the arc external to the nonlinear magnetic insert:**

Assumed *linear* with a map R_N given by:

$$R_N = \pm I \text{ (4x4 identity)}$$

Thus, the phase advance must be $n\pi$.

H_N, I_N are invariant under the one-turn map.

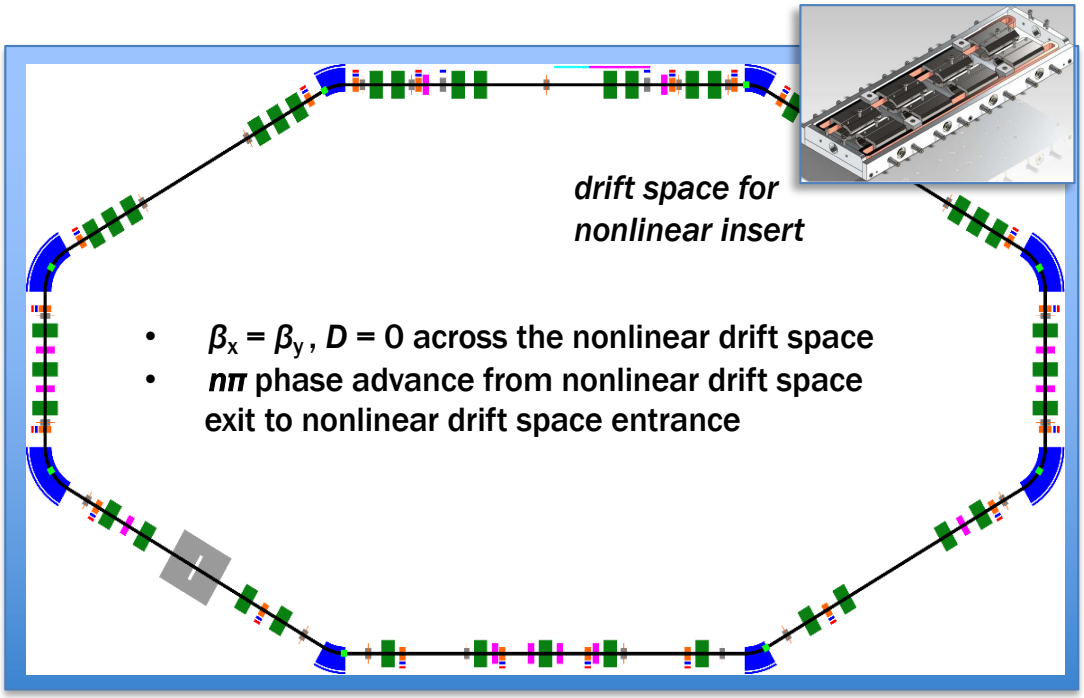

[1] V. Danilov and S. Nagaitsev, Phys Rev Accel Beams **13**, 084002 (2010)

Nonlinear Integrable Optics Lattice Configuration

- **Dynamics inside the nonlinear magnetic insert:**

$$H_\perp = \frac{1}{2}(P_x^2 + P_y^2) - \frac{\tau c^2}{\beta(s)} U\left(\frac{X}{c\sqrt{\beta(s)}}, \frac{Y}{c\sqrt{\beta(s)}}\right) \Rightarrow H_N = \frac{1}{2}(P_{xN}^2 + P_{yN}^2 + X_N^2 + Y_N^2) - \tau U(X_N, Y_N)$$

first invariant

Courant-Snyder transformation, scaling

D&N give in [1] a realizable potential U such that H_N admits a second invariant I_N :

$$\{H_N, I_N\} = 0 \cdot$$

- **Dynamics in the arc external to the nonlinear magnetic insert:**

Assumed *linear* with a map R_N given by:

$$R_N = \pm I \text{ (4x4 identity)}$$

Thus, the phase advance must be $n\pi$.

H_N, I_N are invariant under the one-turn map.

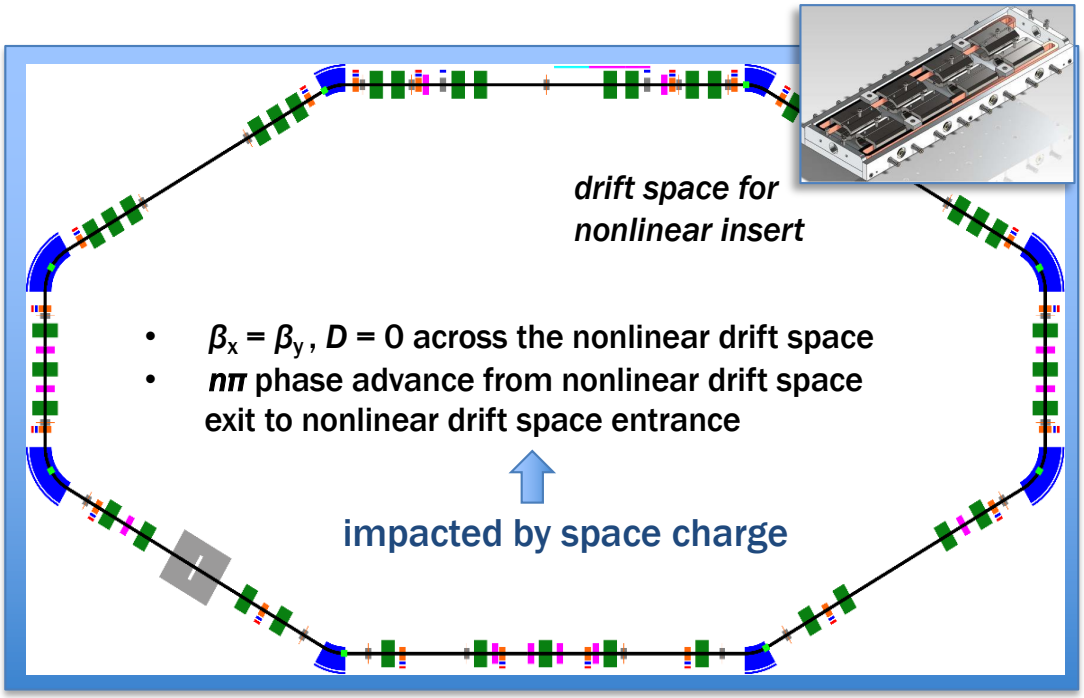

[1] V. Danilov and S. Nagaitsev, Phys Rev Accel Beams **13**, 084002 (2010)

Questions regarding space charge and nonlinear integrable optics in IOTA (using 2.5 MeV protons)

1) Will the presence of space charge destroy the integrability of single-particle motion in IOTA?

2) What are the primary (resonance, other) mechanisms by which this occurs?

3) How does space charge affect the structure of the beam distribution at high current?

4) What consequences will space charge have for beam stability and halo development?

5) How can we address 1)-4) accurately in the presence of numerical artifacts (particle noise)?

- Use *fully symplectic* tracking methods (including self-consistent space charge*).
- Use modeling with high spatial resolution and a large number of particles (≥ 1M).
- Study *reduced dynamical models* to aid in understanding the novel dynamics.
- Use multiple codes and multiple methods to distinguish between integrability and chaos (preservation of invariants, FMA, sensitive dependence on initial conditions).

* J. Qiang, Phys. Rev. ST Accel. Beams 20, 014203 (2017).

General observations regarding nonlinear integrable dynamics and space charge (work by several individuals)

Toy IOTA lattice (arc = linear map)

- perfect integrability without space charge or energy spread
- introducing non-integer tune advance in the arc yields a mixture of regular and chaotic orbits
- chaotic orbits appear near separatrix-like structures or low-order resonances
- nonlinear lattice with space charge shows reduced halo relative to a linearized lattice

Constant focusing channel based on the IOTA nonlinear element

- well-defined Vlasov equilibria (hourglass shape, depressed density in the core)
- rapid relaxation to equilibrium due to phase mixing
- clearly distinct regions of regular and chaotic orbits (bounded)
- regular region shrinks with increasing beam current

Physical lattice with s-dependent focusing

- rapid relaxation to a Vlasov near-equilibrium due to phase mixing
- diffusive spreading on a longer time scale (visible in spread of 2 invariants)
  - a) diffusion of invariants is sensitive to the current and number of simulation particles
  - b) diffusion of invariants decreases if lattice is corrected for coherent SC tune shift
- for weak SC, regular/chaotic regions are similar to those in the IOTA toy lattice with tune error
- halo is reduced when multiple nonlinear inserts are used (SC tune dep. bet. magnets is small)

Lattice, Beam, and Simulation Parameters

- IOTA v. 8.4 lattice –nonlinear integrable optics configuration (1 insert)
  - sextupoles off, RF off –coasting beam
  - drifts, bends, and quads treated through linear order only
  - nonlinear insert treated as ideal (τ = -0.4, c = 0.01 m$^{1/2}$, l = 1.8 m)

- 2.5 MeV proton beam (unbunched)
  - thermal distribution, matched at zero current $f \propto e^{-H/H_0}$
  - zero energy spread to remove chromatic and dispersive effects
  - emittances: ε_{xn} = 0.220 μm, ε_{yn} = 0.466 μm → $\varepsilon_{4D,n}$ = 0.32 μm*
  - beam current is slowly ramped (over 100 turns) to: **5 mA, 8 mA**

- Treatment of space charge
  - IMPACT-Z: 2D symplectic spectral solver, 256×256 modes, 1M particles
  - Boundary $x_{ap} = y_{ap}$ = 5 cm
  - Ensures that space charge fields are smooth and tracking is symplectic.
  - 2K integration steps within the NLI
  - 20 space-charge kicks within the NLI
  - Number of space charge kicks elsewhere chosen to ensure convergence

* Nominal: 0.3 μm, 8 mA from S. Antipov *et al*, JINST 12 T03002 (2017), Table 3

- Structure of the high-intensity proton beam

Matching to the nonlinear lattice at zero current (unbunched coasting beam)

normalized phase space variables (x_N, p_{xN}, y_N, p_{yN})

Thermal beam distribution

$$f \propto e^{-H/H_0}$$

- Hamiltonian is phase-independent
- distribution function is stationary

physical phase space variables (x, p_x, y, p_y)

- Hamiltonian is *s*-dependent
- distribution varies periodically in *s*
- parameter H_0 determines emittance

When τ=0, this is 4D Gaussian.

Beam is matched to the s-dependent nonlinear lattice at the NLI midpoint.

All turn-by-turn data is output at the NLI midpoint.

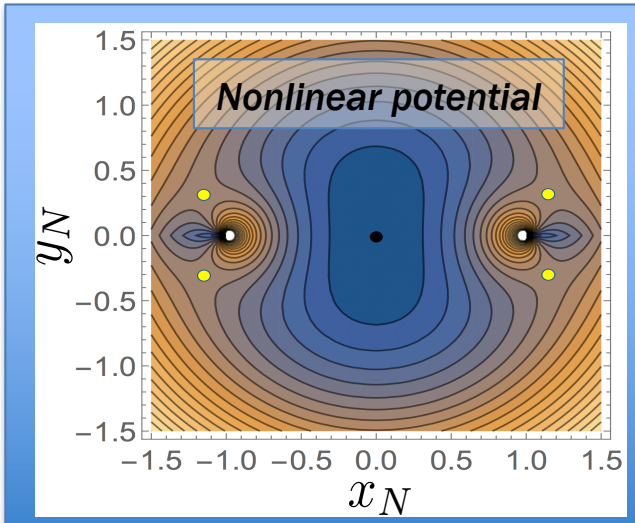

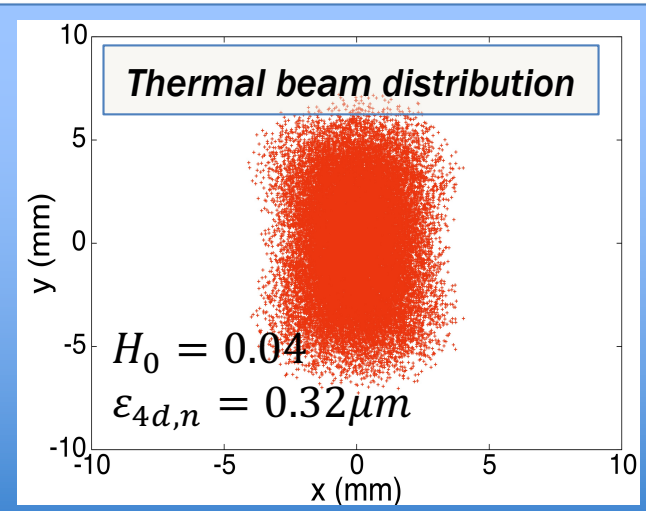

S. Webb *et al*, IPAC 2013 and C. Mitchell *et al*, NOCE 2017.

Beam evolution during adiabatic matching (increasing from 0 - 8 mA over 100 turns)

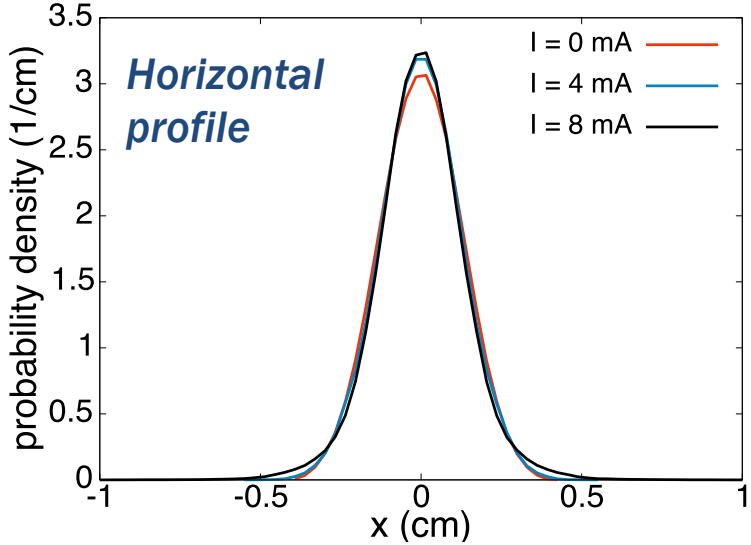

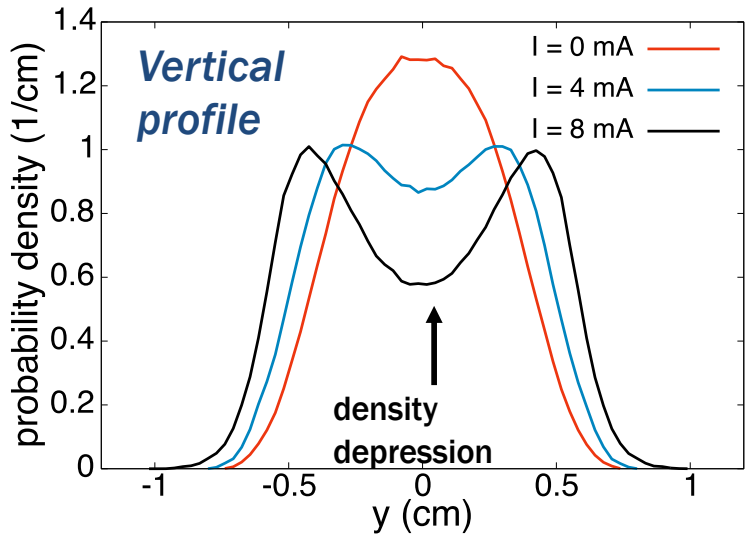

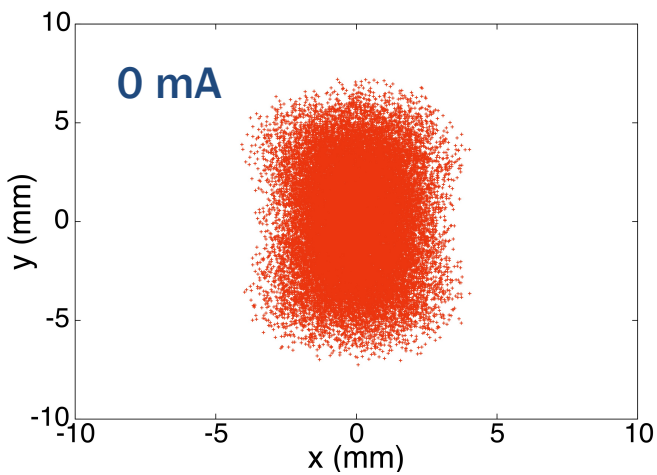

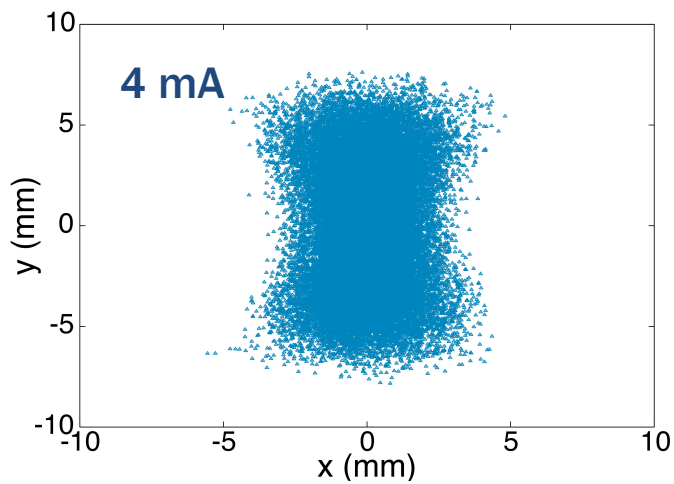

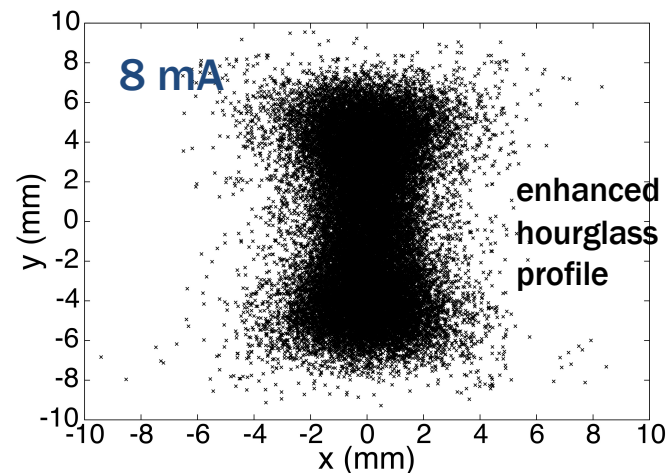

Verification of Adiabatic Matching Procedure

Distance between distributions on successive turns during ramping

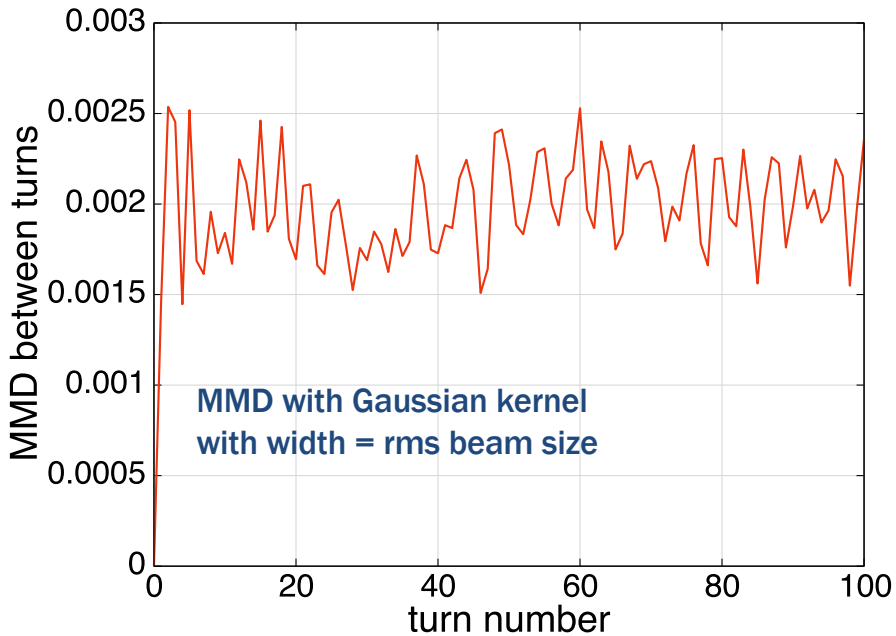

- MMD*: dimensionless measure of distance between arbitrary beam distributions - in the range [0,2]

- Value due to particle noise: $\sqrt{2/N} \approx 1.5 \times 10^{-3}$

- Turn-to-turn distribution evolution is slow (adiabatic).

Beam size evolution after matching (8 mA)

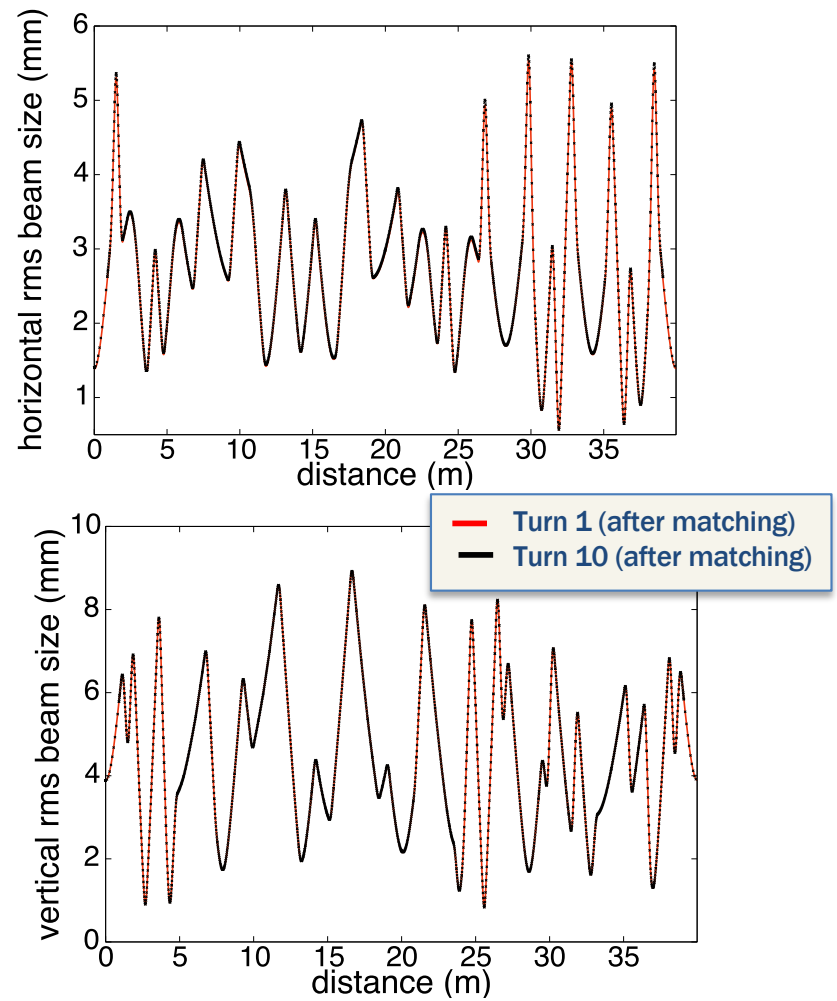

* A. Gretton, J. Mach. Learn. Res. 13, 723-773 (2012)

Structure is similar to Vlasov equilibria constructed in a nonlinear constant focusing channel

Zero current (Λ=0)

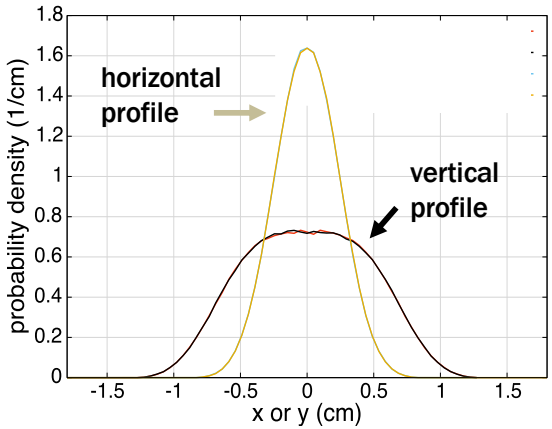

High intensity (Λ=10)

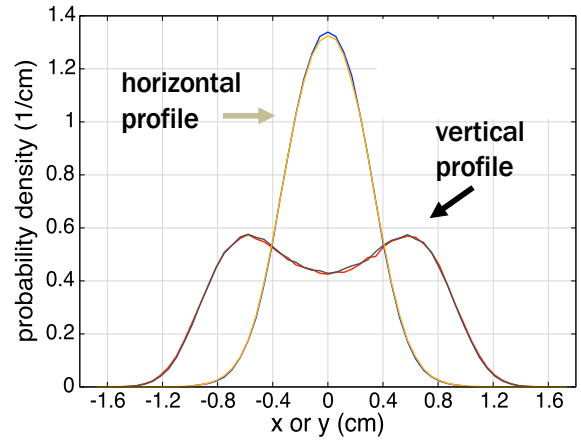

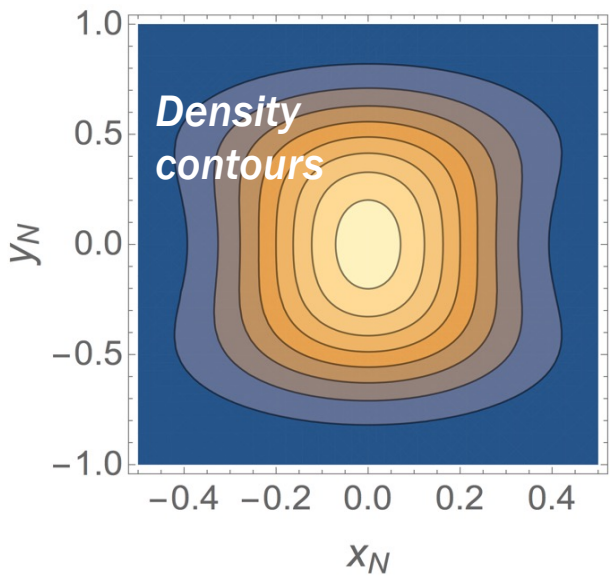

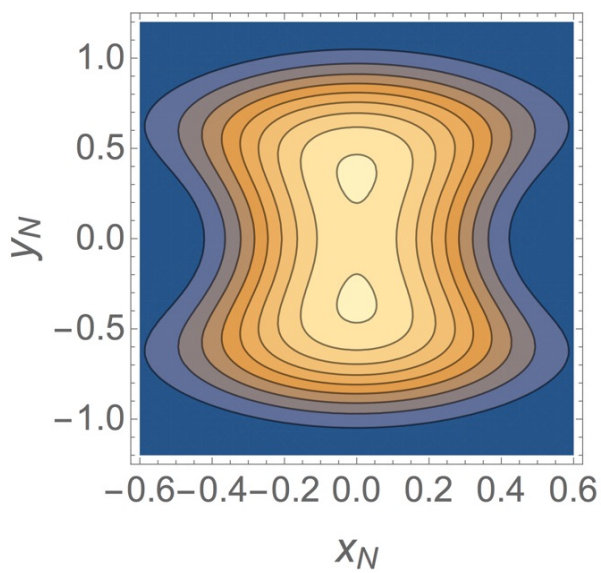

Constant focusing channel based on the IOTA nonlinear potential.

Equilibrium distribution

$$f = G \circ H_N$$

Nonlinear Hamiltonian

$$H_N = \frac{1}{2}\left(p_{xN}^2 + p_{yN}^2\right) + V_0(x_N, y_N) + \Phi_N(x_N, y_N)$$

PDE for the space charge potential

$$\nabla_N^2 \Phi_N = -\Lambda \int_{V_0+\Phi_N}^{\infty} G(h)dh$$

- **2.5 MeV protons**
- **Thermal beam:** $G(h) = \exp(-h/H_0)$
- **NLI parameters and average beta based on the IOTA lattice.**

Comparison for equal 4D emittance.

C. Mitchell *et al*, Phys. Rev. E 100, 053308 (2019) & JINST 15, P07019

- Halo formation and diffusion at high intensity

Halo in the Beam Distribution After 400 Turns (Midpoint of the Nonlinear Insert Element)

Spatial distribution

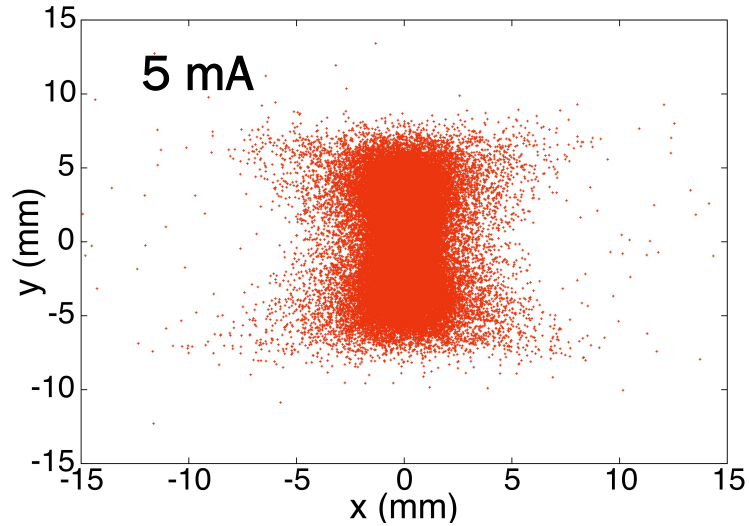

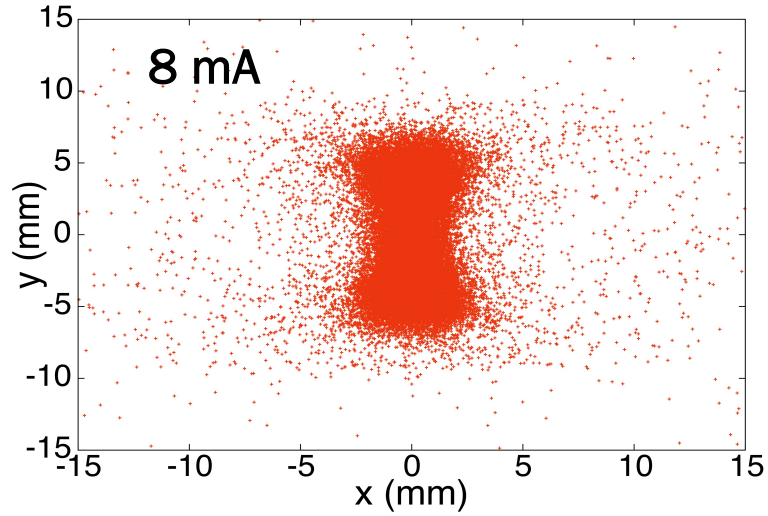

Beam core population remains nearly stationary.

Halo is populated over turns 200-400 (after matching).

At low intensities $\Delta Q_{x,y} << 0.1$ no halo visible after 3,000 turns.

Horizontal profile (log)

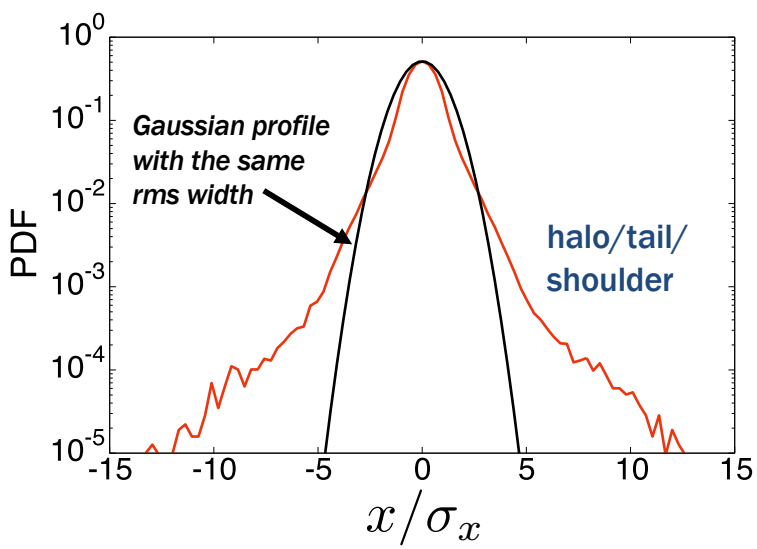

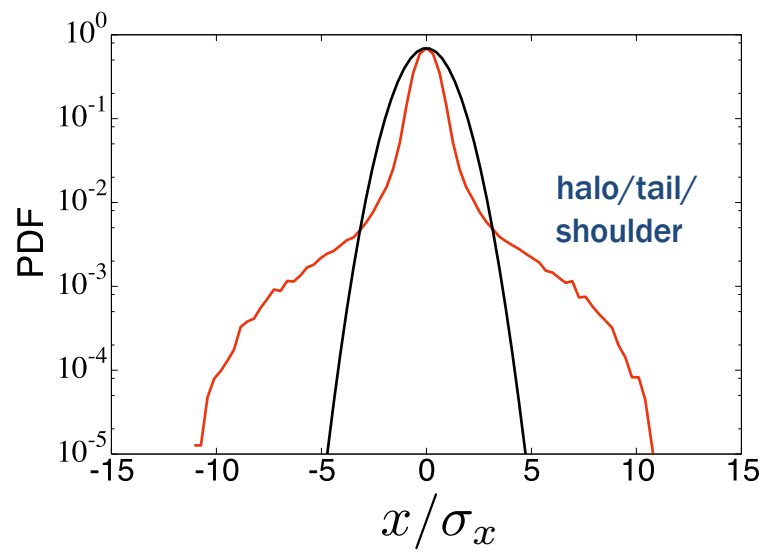

Driven primarily by diffusion in the horizontal plane.

Characterize halo as excess tail population relative to a Gaussian.

Behavior of Orbits Near the Beam Core (8 mA beam)

The turn-by-turn evolution of 2 orbits (blue & black) shown in normalized coordinates.

Phase space projection

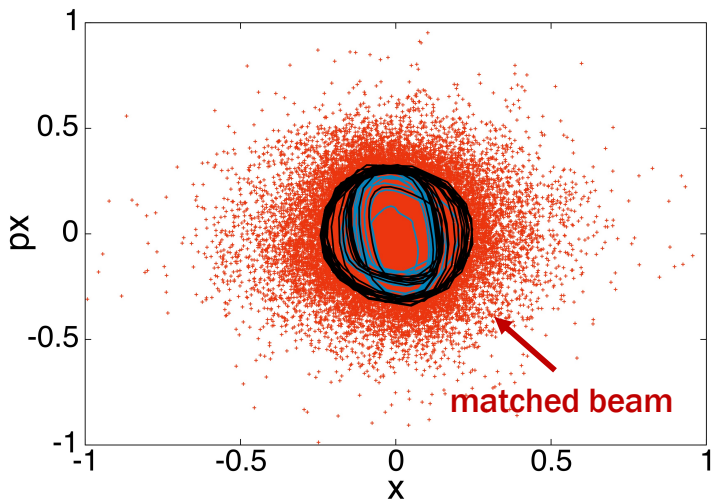

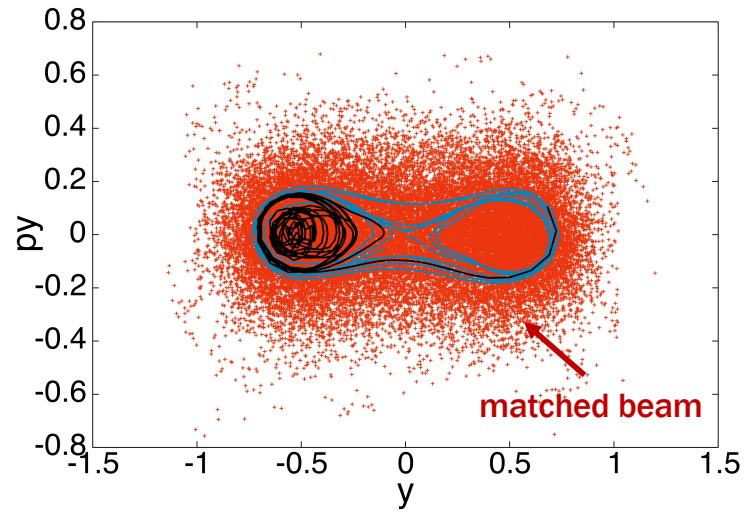

Origin is unstable
In the vertical plane

2 new fixed points near y_N = +/- 0.5

Also observed in the constant focusing model.

Zero-current invariants

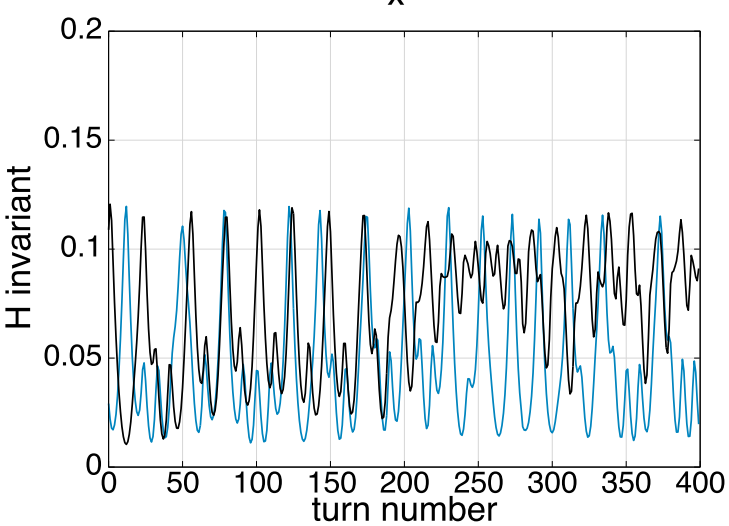

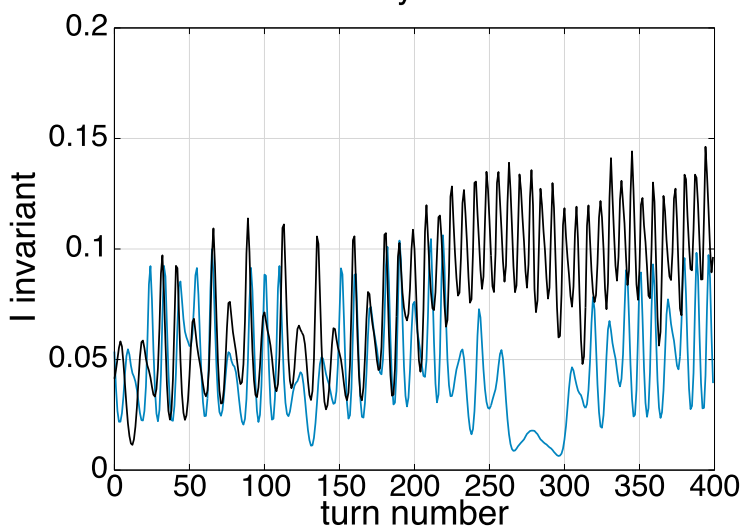

0 mA invariants of motion: (action-like) measure of particle amplitude.

Invariants are bounded < 0.15

Diffusion of Orbits into the Beam Halo (8 mA beam)

The turn-by-turn evolution of 2 orbits (blue & black) shown in normalized coordinates.

Phase space projection

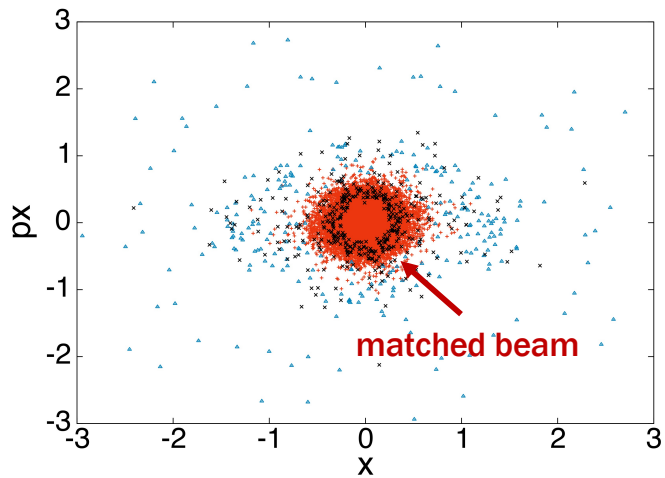

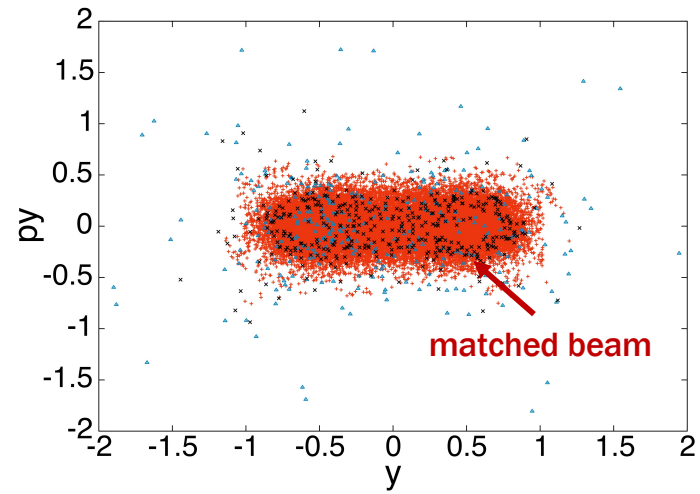

Orbits begin within the beam core with $r \sim 1\sigma_r$

Onset of chaos.

Maximum excursion as large as $x \approx 15\sigma_x$

Zero-current invariants

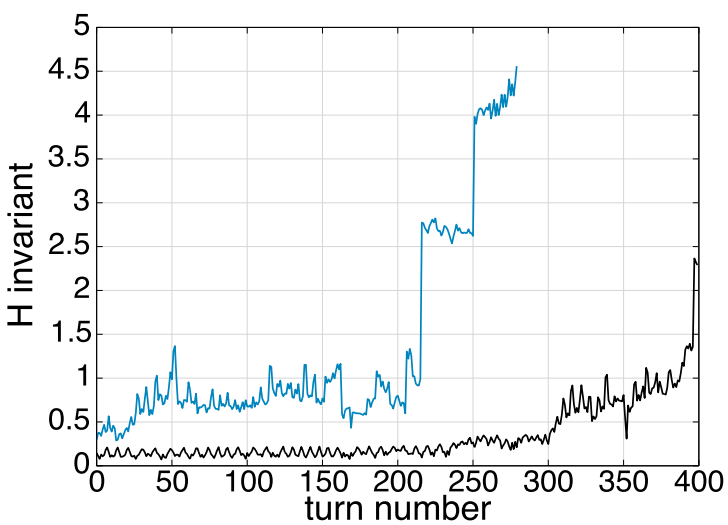

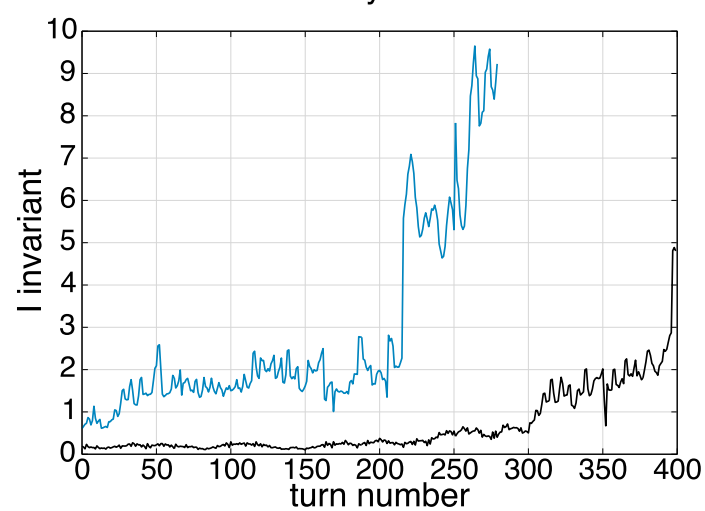

Invariants begin to grow near turn 200.

Particle in blue is lost at large amplitude near turn 270.

Critical and resonance structures in the single-particle phase space (zero current integrable motion)

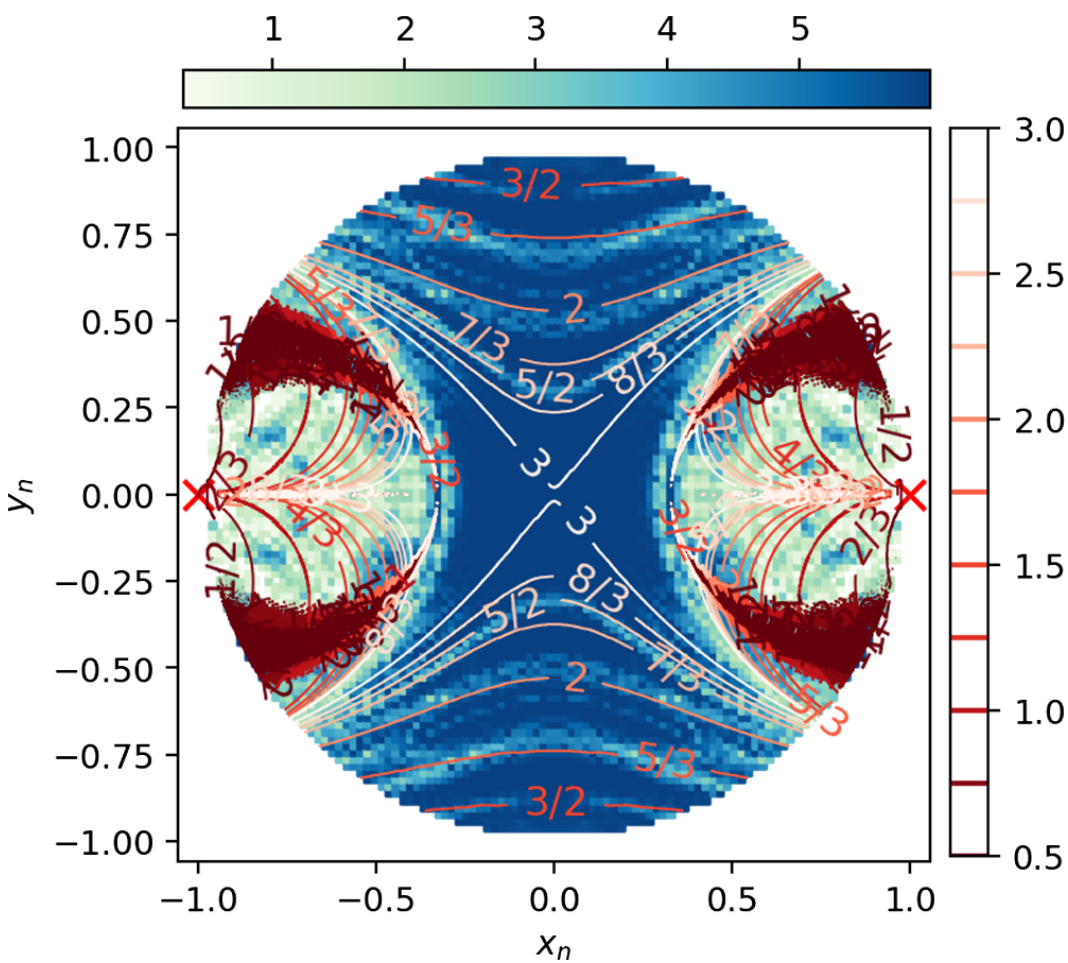

Critical structures:

- Red curve: primary separatrix-like structure
  Black curve: I.C.s for unstable periodic orbits
- Separate regions of distinct orbit behavior
- A matched beam at 0 mA with the nominal emittance lies within the primary separatrix

Resonance structures:

- Resonant contour lines ν_y/ν_x are shown
- High density of resonances outside the primary separatrix
- Color: measure of chaos when phase advance is perturbed (blue = regular)

When the phase advance is depressed, chaos develops first in the region outside the primary separatrix.

K. Hwang *et al*, Phys. Rev. Accel. Beams 23, 084602 (2020)
C. Mitchell *et al*, Phys. Rev. Accel. Beams 23, 064002 (2020)

Critical and resonance structures in the single-particle phase space (zero current integrable motion)

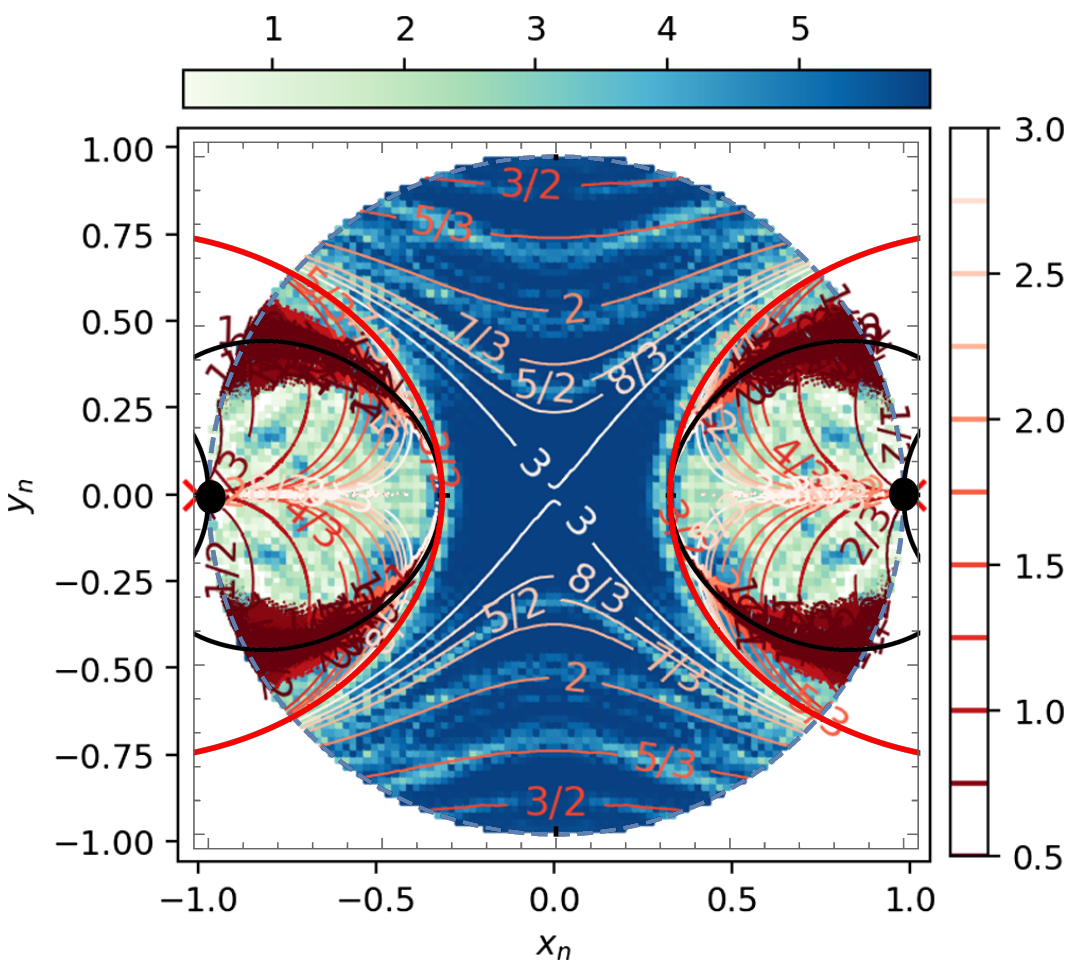

Critical structures:

- Red curve: primary separatrix-like structure
  Black curve: I.C.s for unstable periodic orbits
- Separate regions of distinct orbit behavior
- A matched beam at 0 mA with the nominal emittance lies within the primary separatrix

Resonance structures:

- Resonant contour lines ν_y/ν_x are shown
- High density of resonances outside the primary separatrix
- Color: measure of chaos when phase advance is perturbed (blue = regular)

When the phase advance is depressed, chaos develops first in the region outside the primary separatrix.

K. Hwang *et al*, Phys. Rev. Accel. Beams 23, 084602 (2020)
C. Mitchell *et al*, Phys. Rev. Accel. Beams 23, 064002 (2020)

Spatial Distribution of the Beam in Normalized Coordinates at 5 mA Current

- The spatial distribution is shown in normalized dimensionless coordinates.
- Diffusion is visible along the primary separatrix (red).
- Near the separatrix, the single-particle motion is unstable and sensitive to perturbation.
- A visible fraction of particles moves outside the separatrix → likely chaos.
- Little evidence of significant charge approaching the singular points or branch cuts (black).

Initial distribution (after matching)

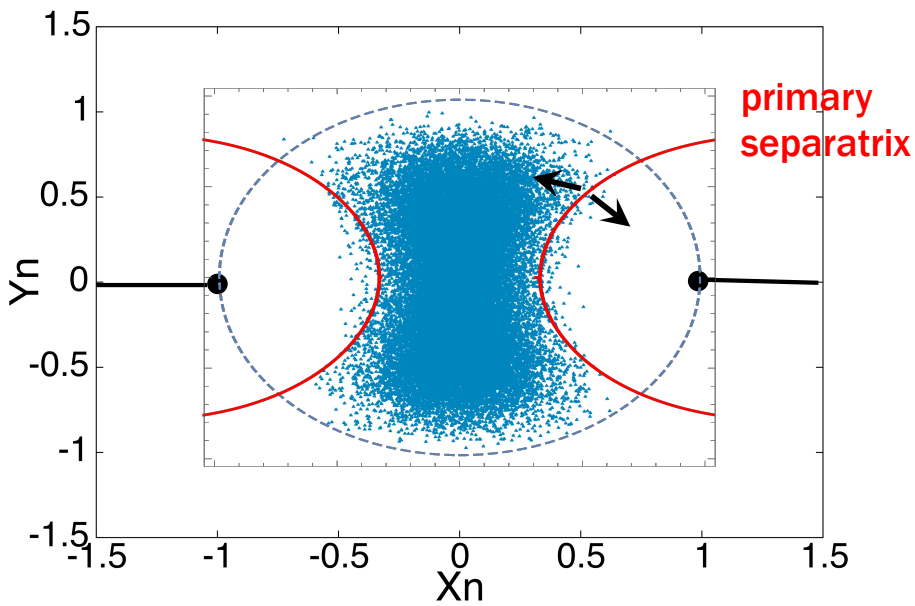

Final distribution (+ 400 turns)

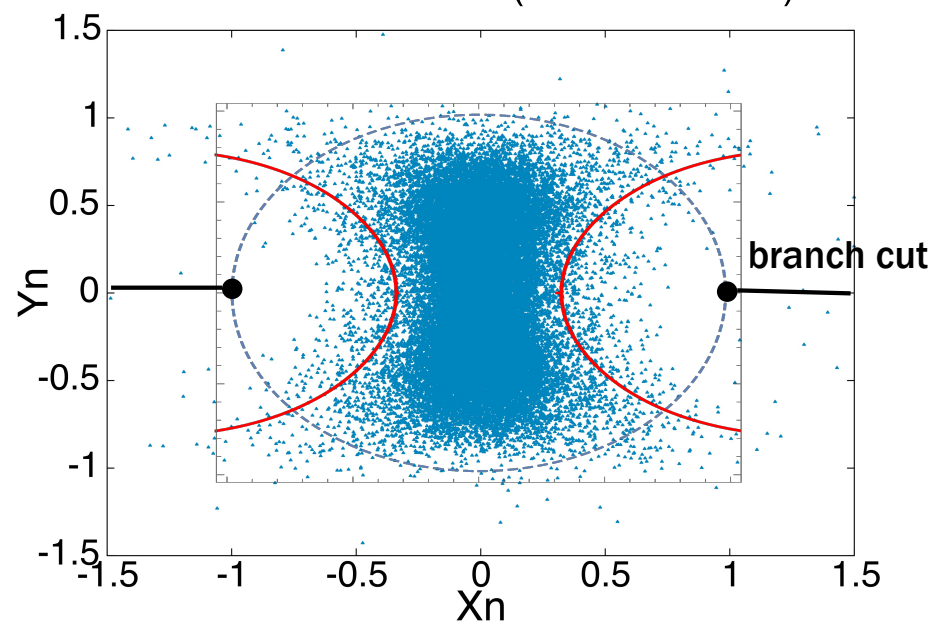

Behavior of the Zero-Current Invariants in the Nonlinear Lattice at 5 mA Current

- Diffusion of zero-current invariants (*H*,*I*) is a consequence of space charge.
- Movement appears to be largely along the primary separatrix (dashed red curve).
- Previous studies have shown that small error in the phase advance can lead to chaos and loss for orbits outside the primary separatrix (in the regions labeled G & C).

Initial distribution (after matching)

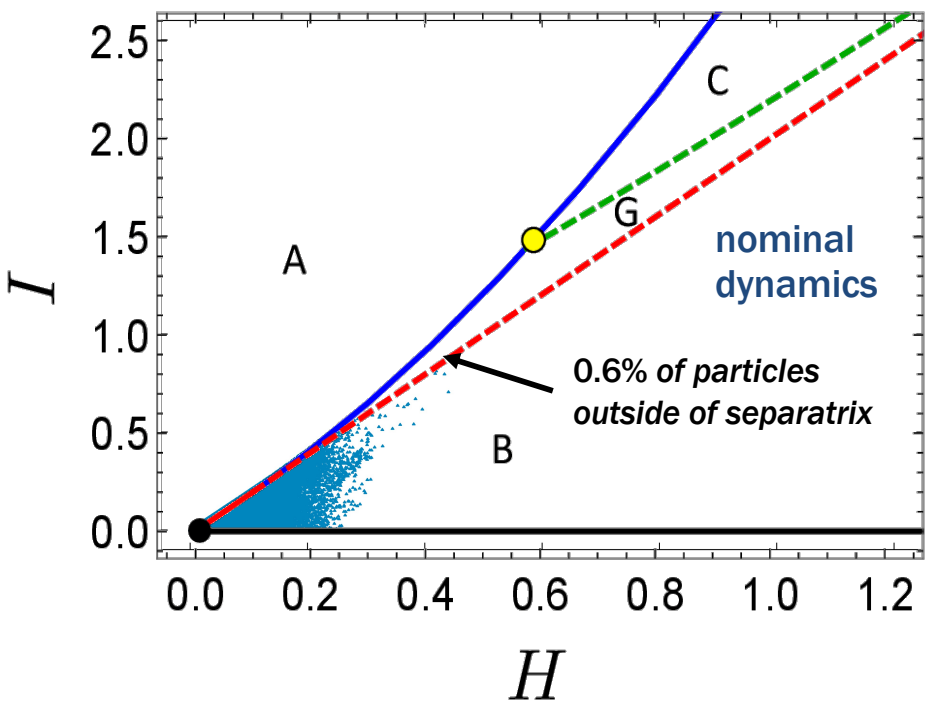

Final distribution (+ 400 turns)

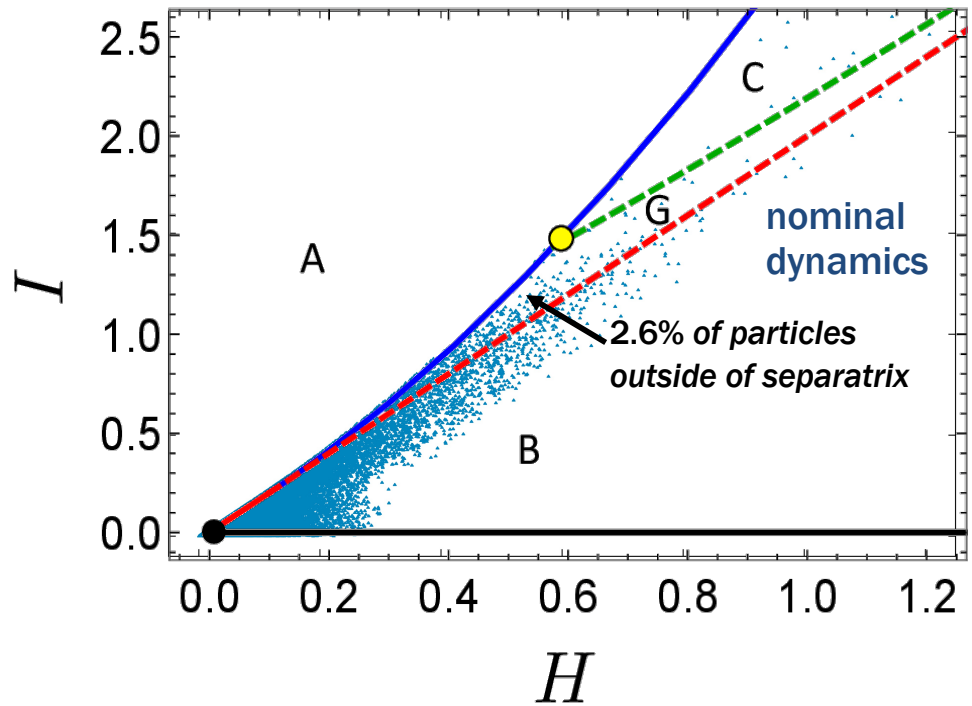

Bifurcation diagram from C. Mitchell *et al*, PRAB 23, 064002 (2020)

Behavior of the Zero-Current Invariants in the Nonlinear Lattice at 8 mA Current

- Diffusion of beam in invariant space (*H*,*I*) is more pronounced at higher intensity (as expected).
- Particles initialized near the primary separatrix (dashed red curve) move toward increasing *H*, *I*, and into regions G and C, associated with significant chaos.
- Two orbits are shown in black—one confined to the core, and one moving into the halo.

Initial distribution (after matching)

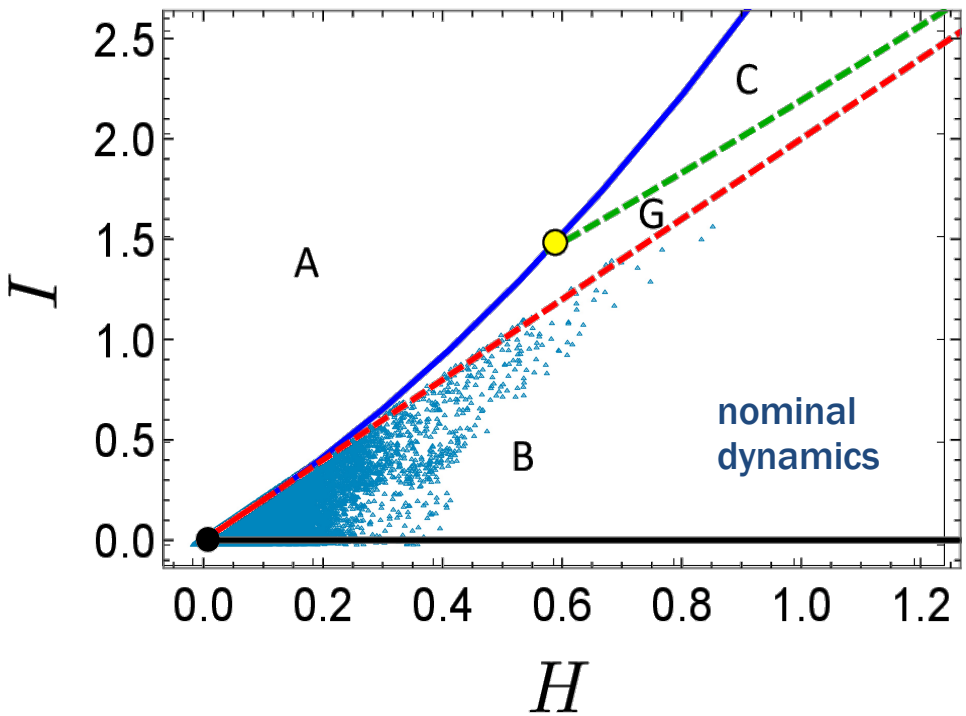

Final distribution (+ 400 turns)

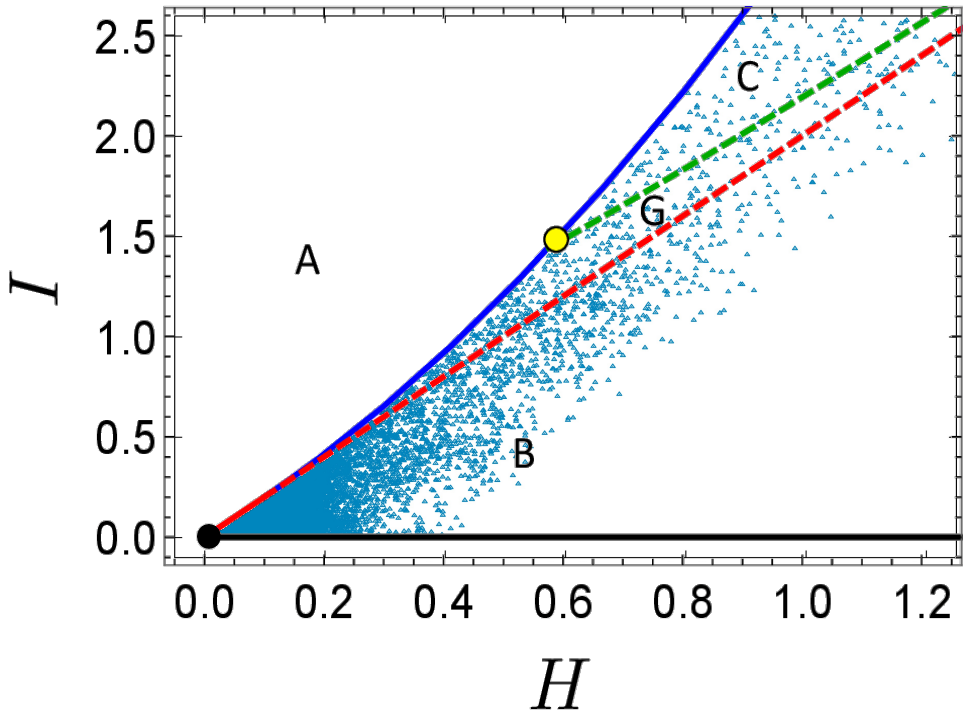

Behavior of the Zero-Current Invariants in the Nonlinear Lattice at 8 mA Current

- Diffusion of beam in invariant space (*H*,*I*) is more pronounced at higher intensity (as expected).
- Particles initialized near the primary separatrix (dashed red curve) move toward increasing *H*, *I*, and into regions G and C, associated with significant chaos.
- Two orbits are shown in black—one confined to the core, and one moving into the halo.

Initial distribution (after matching)

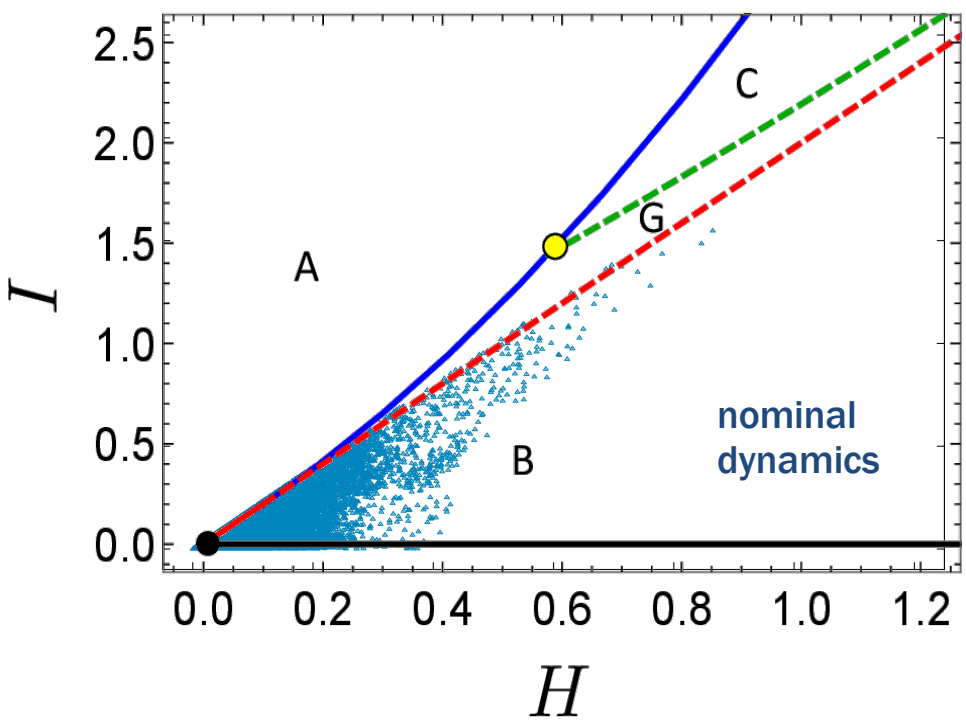

Final distribution (+ 400 turns)

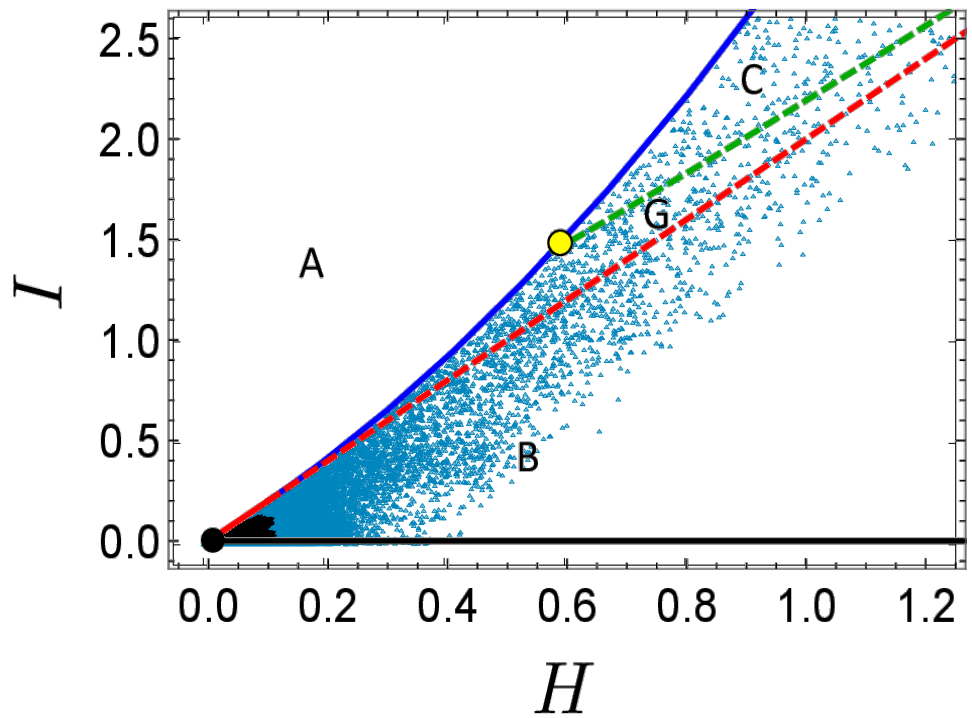

Behavior of the Zero-Current Invariants in the Nonlinear Lattice at 8 mA Current

- Diffusion of beam in invariant space (*H*,*I*) is more pronounced at higher intensity (as expected).
- Particles initialized near the primary separatrix (dashed red curve) move toward increasing *H*, *I*, and into regions G and C, associated with significant chaos.
- Two orbits are shown in black—one confined to the core, and one moving into the halo.

Initial distribution (after matching)

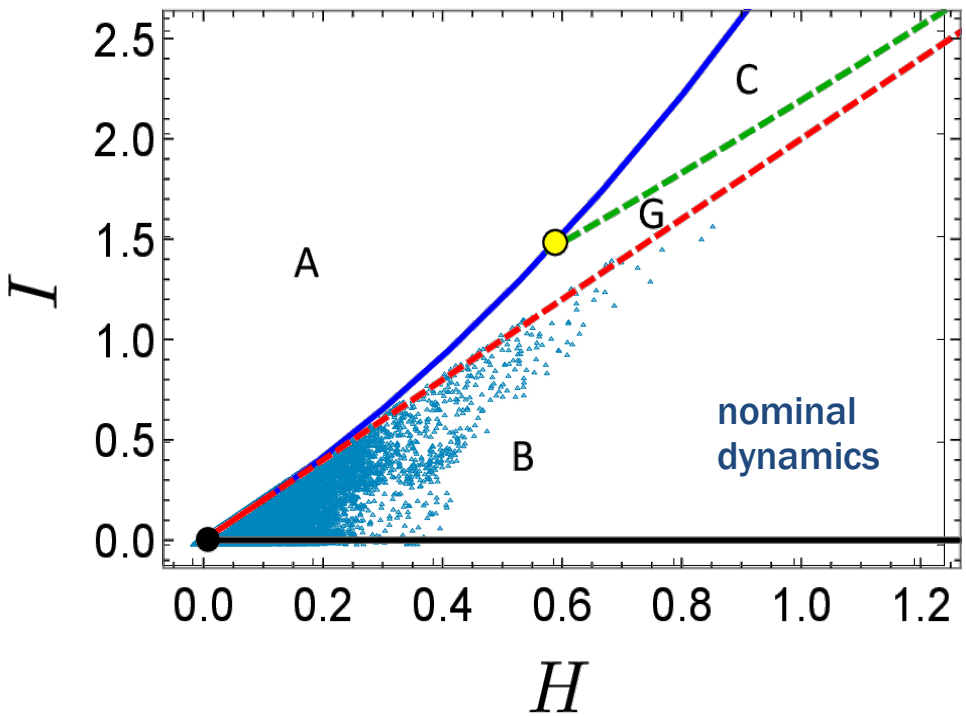

Final distribution (+ 400 turns)

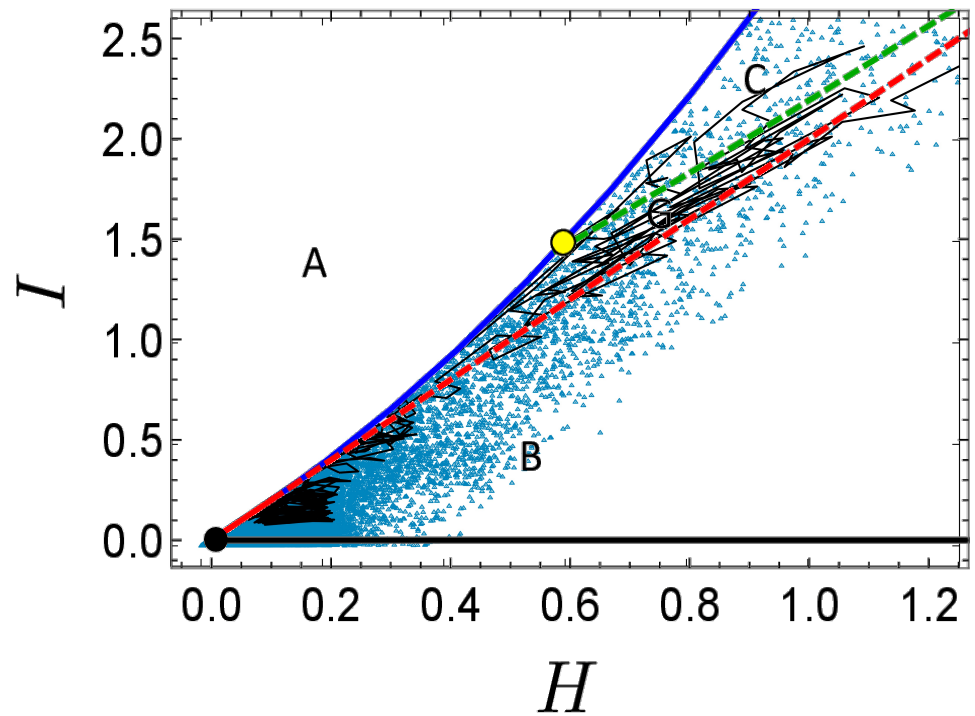

- Mitigation through nonlinear magnet design

Magnetic Vector Potential and Magnetic Field within the IOTA Nonlinear Magnetic Insert

The ideal 2D magnetic field within the nonlinear insert at location s is given by $\vec{B} = \nabla \times \vec{A} = -\nabla\psi$, where the potentials are given in terms of dimensionless quantities:

$$F = \frac{A_s + i\psi}{B\rho}, \quad z = \frac{x + iy}{c\sqrt{\beta(s)}}, \quad \tilde{t} = \frac{\tau c^2}{\beta(s)}$$

using the complex function:

$$F(z) = \left(\frac{\tilde{t}z}{\sqrt{1-z^2}}\right)\arcsin(z) \ .$$

The transverse focusing fields vary longitudinally with s:

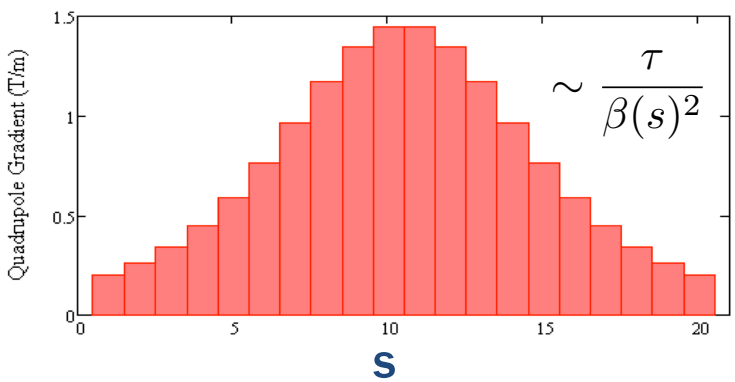

Field lines of the nonlinear insert in the transverse plane (blue)

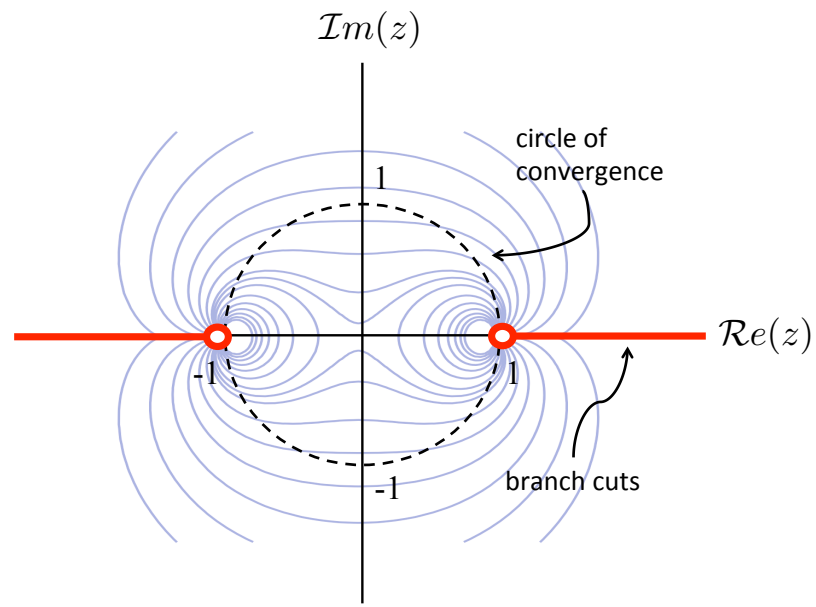

τ – dimensionless insert strength
c – transverse scale parameter [$m^{1/2}$]
$B\rho$ – magnetic rigidity [T-m]
β – betatron amplitude [m]

Magnetic Vector Potential and Magnetic Field within the IOTA Nonlinear Magnetic Insert

The ideal 2D magnetic field within the nonlinear insert at location s is given by $\vec{B} = \nabla \times \vec{A} = -\nabla\psi$, where the potentials are given in terms of dimensionless quantities:

$$F = \frac{A_s + i\psi}{B\rho}, \quad z = \frac{x + iy}{c\sqrt{\beta(s)}}, \quad \tilde{t} = \frac{\tau c^2}{\beta(s)}$$

using the complex function:

$$F(z) = \left(\frac{\tilde{t}z}{\sqrt{1-z^2}}\right)\arcsin(z) \ .$$

Singular points in the transverse plane:

$$x_\infty = \pm c\sqrt{\beta(s)}$$

Field lines of the nonlinear insert in the transverse plane (blue)

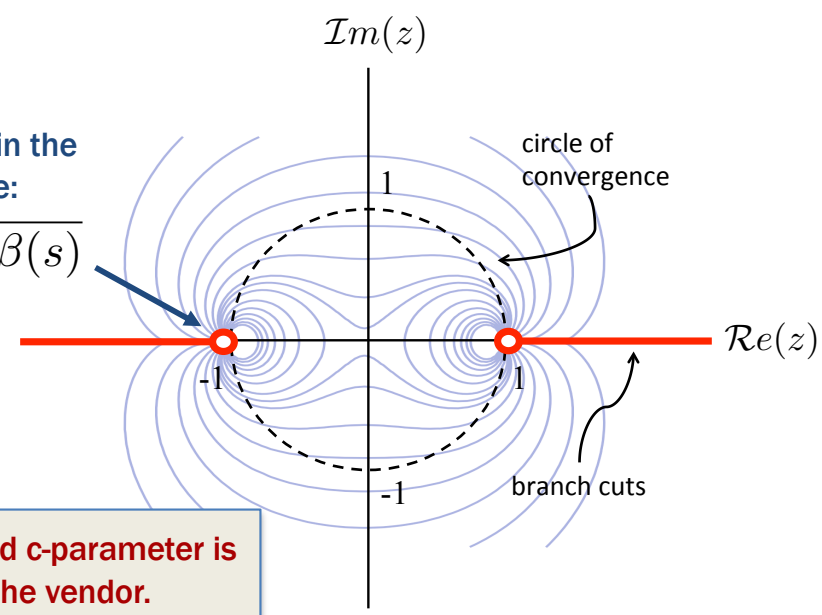

The transverse focusing fields vary longitudinally with s:

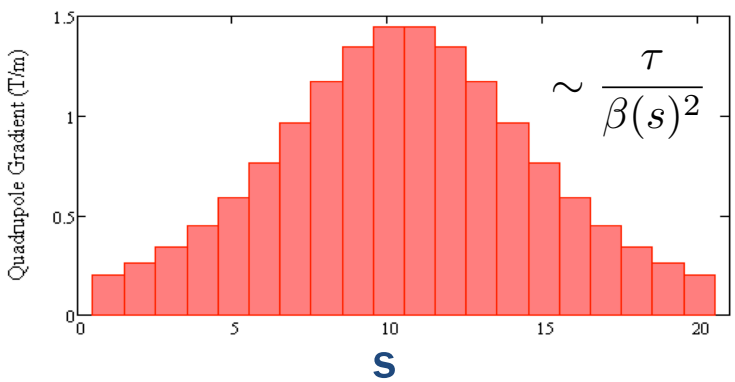

Design with increased c-parameter is being explored with the vendor.

Moves singular points away from the axis & increases transverse aperture.

Affects all multipoles > quadrupole.

τ – dimensionless insert strength
c – transverse scale parameter [$m^{1/2}$]
$B\rho$ – magnetic rigidity [T-m]
β – betatron amplitude [m]

Effect of the Increasing the c Value on the Matched Beam Distribution in Invariant Space

5 mA, nominal emittance
(matched distribution for several c)

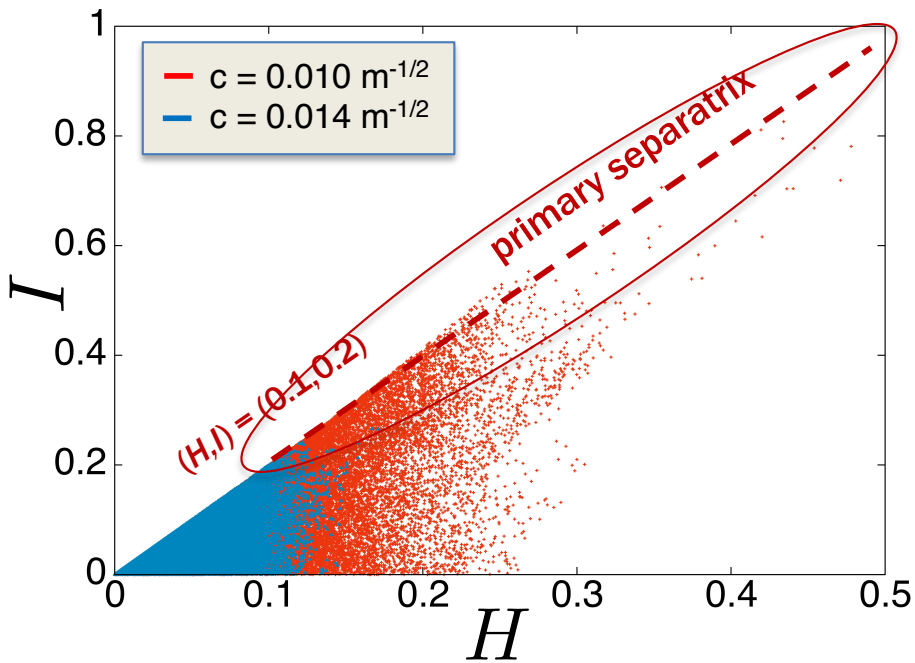

8 mA, nominal emittance
(matched distribution for several c)

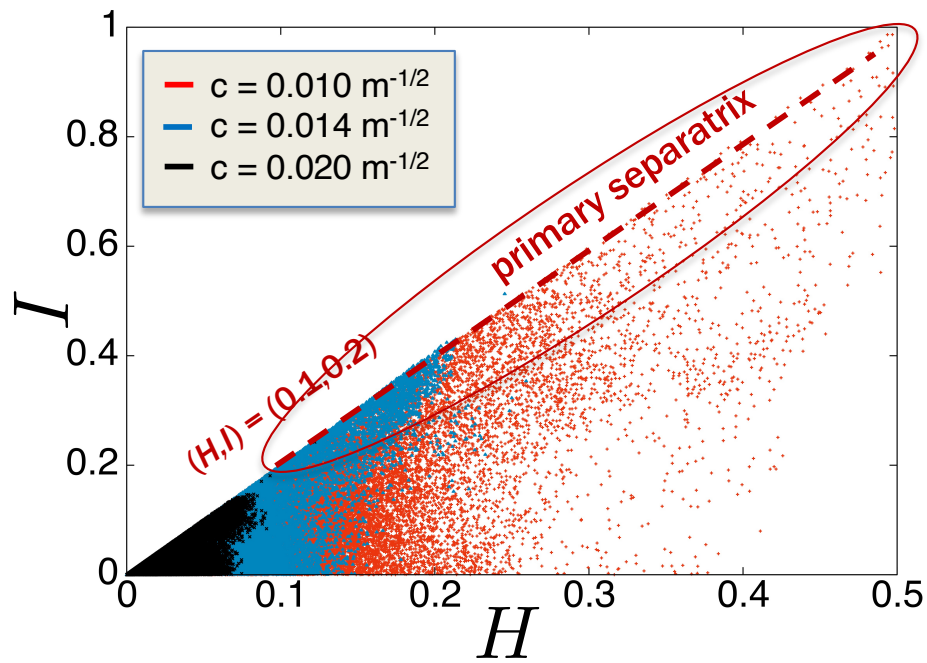

- Increasing the c value leads the beam footprint to shrink in invariant space.
- The primary separatrix begins at (H,I)=(0.1,0.2) and extends along the ray I = 2H
- For sufficiently large c, the beam can be confined away from the primary separatrix.

Initial Distribution (After Adiabatic Matching) at 5 mA Current for Two Distinct Values of c

The spatial distribution is shown in normalized dimensionless coordinates for comparison with critical structures.

Matched distribution
(c = 0.01 $m^{1/2}$)

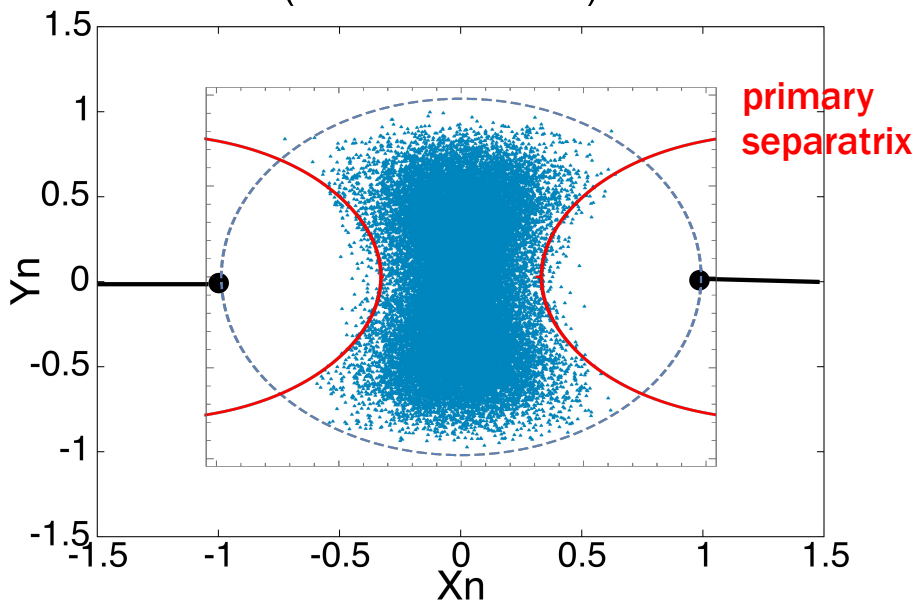

Matched distribution
(c = 0.014 $m^{1/2}$)

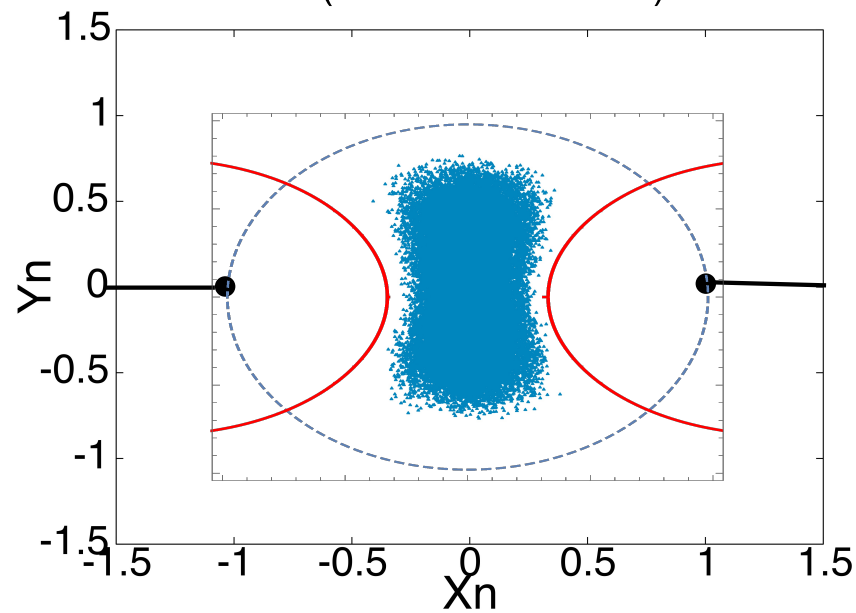

$\varepsilon_{x,n} = 0.24\ \mu m$
$\varepsilon_{y,n} = 0.52\ \mu m$
$\varepsilon_{4D,n} = 0.35\ \mu m$

← similar emittance →

$\varepsilon_{x,n} = 0.22\ \mu m$
$\varepsilon_{y,n} = 0.52\ \mu m$
$\varepsilon_{4D,n} = 0.34\ \mu m$

Horizontal Beam Diffusion is Significantly Reduced by Increasing the Magnetic Insert c Value

- The beam size is shown once per turn, at the midpoint of the nonlinear magnetic insert element.
- The turn count begins after adiabatic matching.

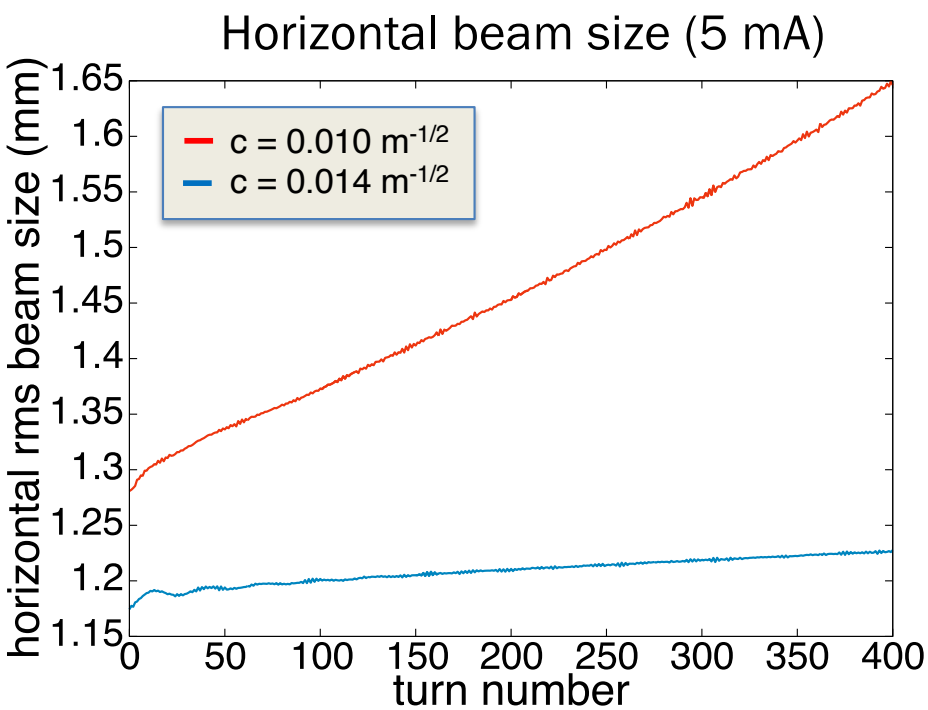

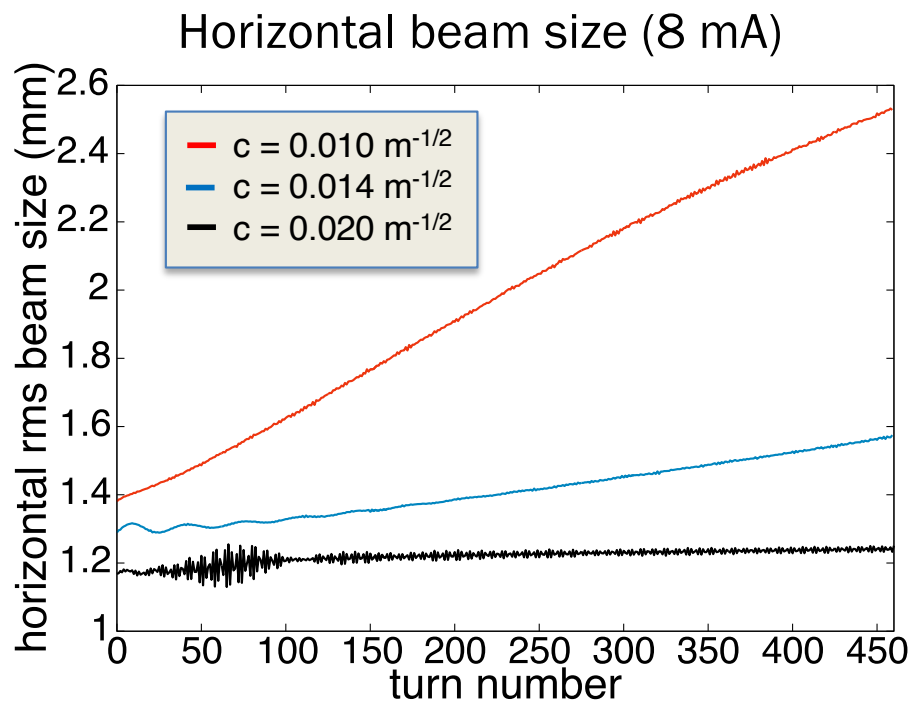

The effect of diffusion on the vertical beam size is much smaller (not shown).
The physical horizontal aperture at the midpoint of the existing magnetic insert element is X_{ap} = 4 mm.

Beam Halo in the Final Distribution (After 400 Turns) at 5 mA for Increasing Values of c

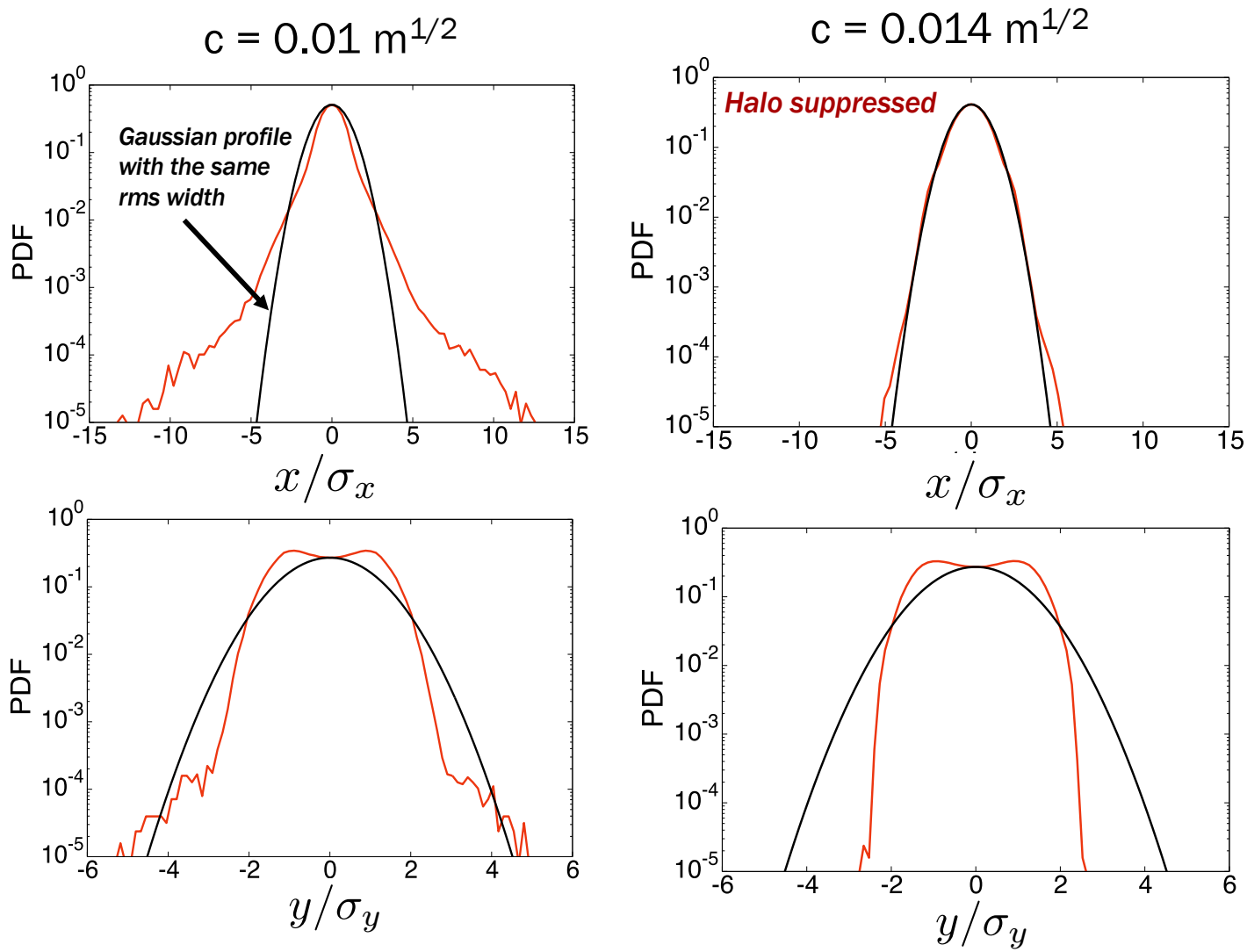

- Both beams are initialized using adiabatic matching.
- Initial emittance near the nominal value.
- Halo visible in the horizontal profile is strongly suppressed.
- The small visible halo in the vertical profile is also suppressed.

Beam Halo in the Final Distribution (After 400 Turns) at 8 mA for Increasing Values of c

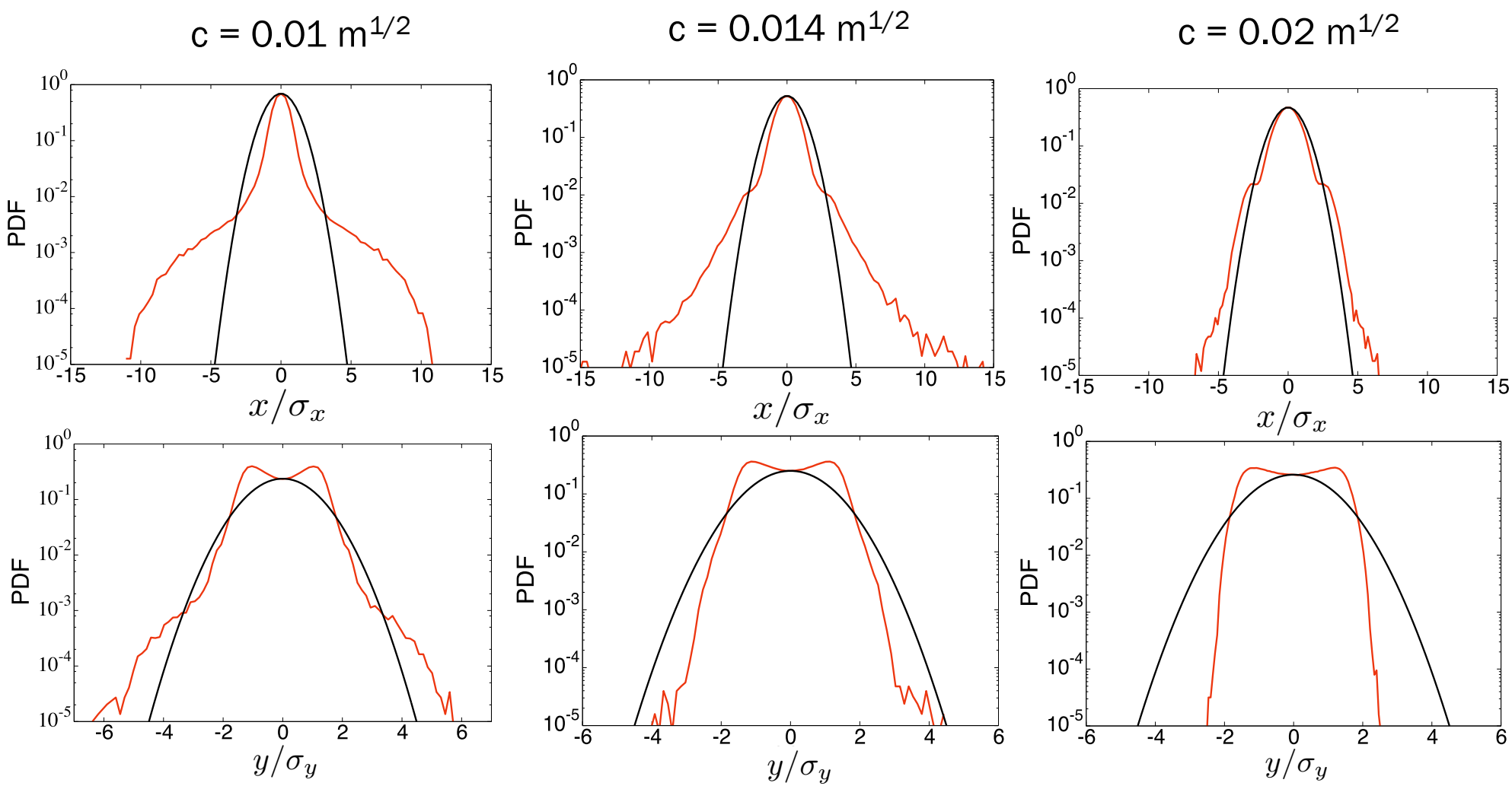

Beam Halo in the Final Distribution (After 400 Turns) at 8 mA for Increasing Values of c

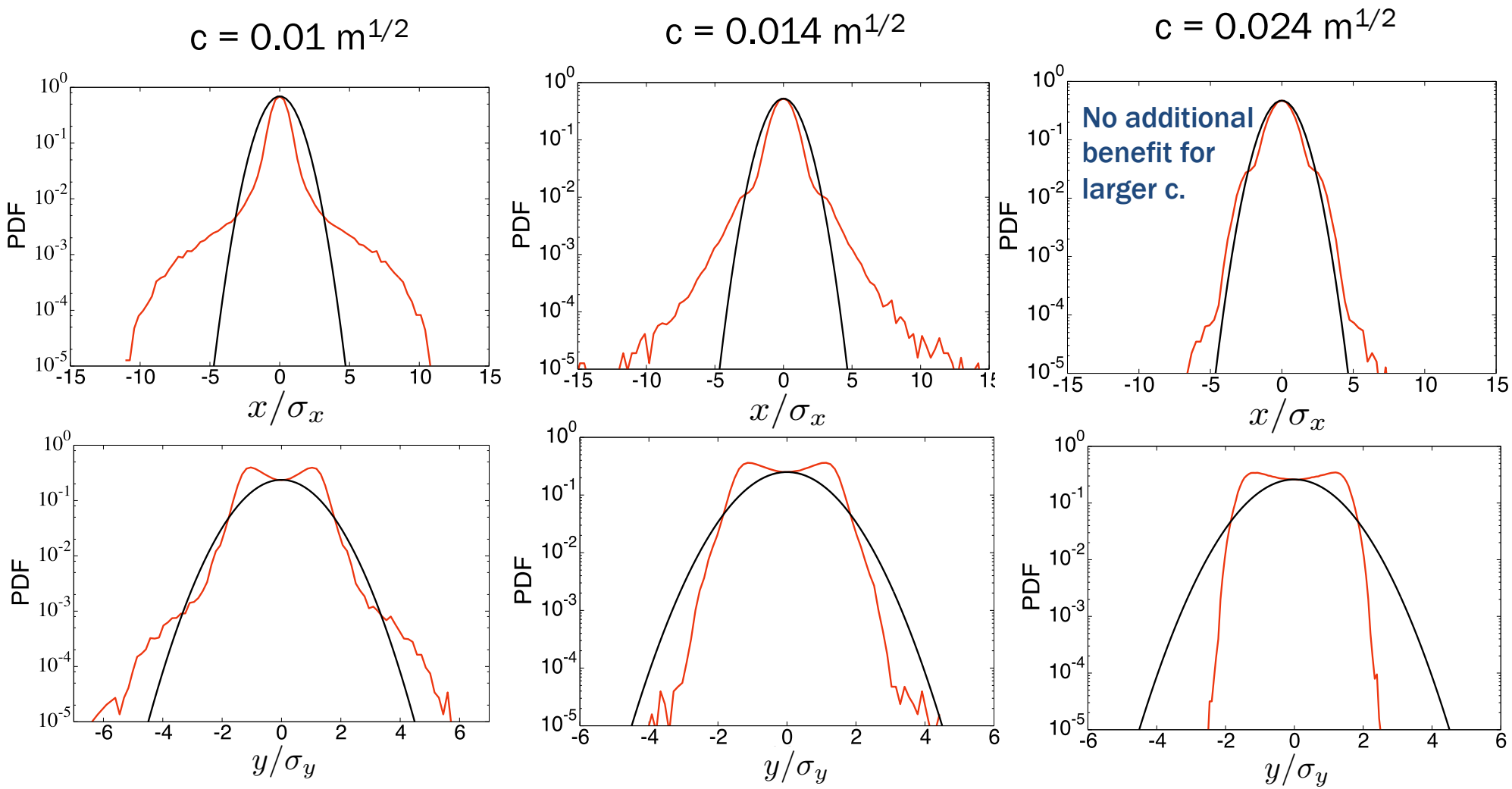

Conclusions

- Due to the novel structure of the nonlinear integrable focusing, care is taken in modeling intense space charge to minimize numerical artifacts and sources of simulation noise.
- Adiabatic matching appears to work well for beam initialization. The matched high-intensity beam is qualitatively similar to that seen in a nonlinear constant focusing lattice.
- Some halo development occurs in the nonlinear integrable lattice at high intensity. This appears to be driven by chaotic diffusion associated with crossing a critical structure in the phase space ("primary separatrix").
- This can be mitigated by increasing the magnetic insert c-value to confine the beam away from critical phase space structures. Additional benefit could be gained by using multiple nonlinear insert elements to reduce the phase advance between passes (as in an RCS).
- Detailed properties of the nonlinear integrable Hamiltonian (*eg*, critical and resonant structures) play an important role when the system is perturbed → further exploring the space of possible integrable focusing schemes could have major impact on beam performance at high intensity.